Avalanching glacier instabilities: Review on processes and early warning perspectives

Jerome Faillettaz, Martin Funk, Christian Vincent

AGU PUBLICATIONS

Reviews of Geophysics

REVIEW ARTICLE

10.1002/2014RG000466

Key Points:
- A review of the different types of rupture mechanisms is provided
- The physical processes leading to the instabilities are described
- Early warning perspectives are discussed

Correspondence to:
J. Faillettaz,
jerome.faillettaz@geo.uzh.ch

Citation:
Faillettaz, J., M. Funk, and C. Vincent (2015), Avalanching glacier instabilities: Review on processes and early warning perspectives, *Rev. Geophys.*, *53*, 203–224, doi:10.1002/2014RG000466.

Received 8 JUL 2014
Accepted 5 MAR 2015
Accepted article online 14 MAR 2015
Published online 15 MAY 2015

Avalanching glacier instabilities: Review on processes and early warning perspectives

Jérome Faillettaz[1,2], Martin Funk[1], and Christian Vincent[3]

[1]Laboratory of Hydraulics, Hydrology and Glaciology, ETH Zurich, Zurich, Switzerland, [2]Also at 3G, Department of Geography, University of Zurich, Zurich, Switzerland, [3]Laboratoire de Glaciologie et Géophysique de l'Environnement UMR 5183, Grenoble, France

Abstract Avalanching glacier instabilities are gravity-driven rupture phenomena that might cause major disasters, especially when they are at the origin of a chain of processes. Reliably forecasting such events combined with a timely evacuation of endangered inhabited areas often constitute the most efficient action. Recently, considerable efforts in monitoring, analyzing, and modeling such phenomena have led to significant advances in destabilization process understanding, improving early warning perspectives. The purpose of this paper is to review the recent progress in this domain. Three different types of instabilities can be identified depending on the thermal properties of the ice/bed interface. If cold (1), the maturation of the rupture is associated with a typical time evolution of surface velocities and passive seismic activity. A prediction of the final break off is possible using these precursory signs. For the two other types, water plays a key role in the development of the instability. If the ice/bed interface is partly temperate (2), the presence of meltwater may reduce the basal resistance, which promotes the instability. No clear and easily detectable precursory signs are known in this case, and the only way to infer any potential instability is to monitor the temporal evolution of the thermal regime. The last type of instability (3) concerns steep temperate glacier tongues switching for several days/weeks during the melting season into a so-called "active phase" followed in rare cases by a major break-off event. Although the prediction of such events is still far from being achievable, critical conditions promoting the final instability can be identified.

1. Introduction

Breaking off of ice at the edge of a glacier is termed ice calving. Most of these events occur for ocean or lake terminating glaciers. Calving in the case of glaciers without any contact with a water body is less known. This is referred to as dry calving and may occur at the terminus of so-called avalanching glaciers [*Pralong and Funk*, 2006]. Avalanching glaciers are defined as glaciers lying on a sufficiently steep slope so that detaching ice chunks can fall away from the glacier terminus and give rise to ice avalanches.

Dry calving occurs when ice at the glacier front is no longer able to support its own weight: a gravity-driven rupture phenomenon. Although relatively rare, they can lead to major disasters, especially when they are at the origin of a chain of processes involving other materials such as snow (snow avalanche), water (flood), and/or debris (mudflow). The most tragic and destructive event occurred in the Peruvian Andes in 1962 and 1970 at Mount Huascaran. In 1962, a huge ice/snow avalanche penetrated 16 km into the Santa Valley, destroying nine villages and killing more than 4000 people. In 1970, at the same location an earthquake triggered another ice avalanche of an estimated volume of 10^7 to 10^8 m^3. This avalanche reached the city of Yungay and killed around 20,000 people [*Lliboutry*, 1975]. More recently, on 20 September 2002 an enormous rock/ice avalanche and subsequent mudflow was reported in the Kazbek massif, Northern Ossetia, Russian Caucasus. After sliding for some 30 km in the valley, the debris/mud flow killed more than 120 people [*Haeberli et al.*, 2004; *Huggel et al.*, 2005; *Evans et al.*, 2009]. In the Alps, one of the most tragic events occurred in 1965 in Switzerland when the terminal part of the Allalingletscher broke off, killing 88 employees at the Mattmark dam construction site [*Röthlisberger*, 1981].

In general, events involving a chain of processes are difficult to detect at an early stage. To protect the population against such events, a timely evacuation constitutes often the only efficient way to secure the potentially endangered area. For this reason, a reliable forecast of such calving events is desirable.

Unfortunately, this remains a challenge, as the physical processes involved are not yet fully understood.

In this context, scientists have to cope with problems of different natures:

1. The heterogeneous nature of both the material involved in the instability—i.e., ice (e.g., microcracks and ice crystals) and the ice-bedrock contact.
2. The difficulties in characterizing and measuring such heterogeneities at all scales.
3. The nonlinearity of rupture processes that involves these heterogeneities.
4. The nature of the driving force leading to the catastrophic rupture of the glacier: the rupture can either be triggered by quasi-static internal changes, such as damage accumulation in the ice, or by external effects such as earthquakes or rapid changes of the subglacial water flow regime.

Several calving studies have been performed for glaciers terminating in water with the aim to obtain a general calving "law" capable of quantifying calving rates [*Benn et al.*, 2007a, and references therein], which is an important issue in the context of sea level rise projections [*Moore et al.*, 2013]. Proposed theoretical calving frameworks are semiempirical [*Van der Veen*, 2002; *Benn et al.*, 2007a; *Alley et al.*, 2008] or based on statistical physics [*Bassis*, 2011] or on concepts of self-organized critical systems [*Åström et al.*, 2014]. The focus of our study is a forecast of the size and the time of failure of individual dry calving events. This is of minor importance for the determination of the calving rate of a glacier terminating in a water body, because the relevant spatial and temporal scales are different in both cases. Furthermore, the presence or the absence of a water body at the terminus gives rise to different processes controlling calving dynamics of the glacier.

The destabilization of ice chunks at the edge of a glacier depends on fracture processes within the ice and on the stresses in the fracture zone. The stress in the fracture zone, in turn, depends on the glacier geometry, the ice rheology, and basal motion. The stress magnitude in the fracture zone of avalanching and tidewater glaciers is similar and can reach values up to 300 kPa [*Reeh*, 1968; *Van der Veen*, 1999; *Hanson and Hooke*, 2000; *Pralong and Funk*, 2006; *Todd and Christoffersen*, 2014; *Cook et al.*, 2014; *Krug et al.*, 2014]. At this stress regime, the fracture process is expected to be similar in dry and wet calving conditions and consists of microcrack accumulation over several weeks [*Mahrenholtz and Wu*, 1992; *Pralong and Funk*, 2005], a process termed subcritical crevassing [*Weiss*, 2004]. The final break off or calving occurs when crevasses have penetrated the entire ice thickness [*Benn et al.*, 2007a]. The final crack propagation to the glacier base in the case of wet calving might be accelerated by partial water filling of the crevasses [*Van der Veen*, 2002], which is rather unlikely in the case of high-altitude avalanching glaciers with little surface melt.

Ice fracture processes are mainly controlled by strain rates resulting from the glacier flow field in the fracture zone, which crucially depends on basal motion [*Benn et al.*, 2007b]. While glacier flow in the case of wet calving is always dominated by basal motion, dry calving glaciers are subject to very different basal motion conditions, varying from negligible sliding to nearly surge conditions within 2–3 weeks of failure in certain cases and no sliding at all in others [*Röthlisberger*, 1981]. This indicates that the propagation of fractures is expected to evolve in a different way for tidewater and avalanching glaciers.

The focus of the research activities on tidewater glacier calving is dominated by the pressing need for practical and robust parameterizations in prognostic ice sheet models and sea level studies. In this context it is not necessary to model individual calving events but to capture the problem with an appropriate large-scale modeling strategy. For predicting individual calving events from avalanching glaciers, small-scale processes become important. In this case, the frequency and volume determination of ice avalanches are crucial especially in densely populated areas.

The aim of this review is an improved description of the onset of the instability, the maturation of the rupture process, and the influence of water as a triggering mechanism leading to the final rupture. The ultimate goal is to provide valuable tools for an accurate time prediction of a critical breaking off event.

Once classified, each type of glacier instability will be analyzed and discussed with the help of examples. Although glacier instabilities are universal phenomena occurring all over the world, it appears that the only relevant experimental studies to explain and illustrate the mechanisms at work in each type of instability was performed on alpine glaciers. These mechanisms as well as possible prediction strategies are reviewed and discussed. These analyses are based on different results, such as field measurements (mainly surface displacements and seismic surveys) as well as numerical modeling of the instability evolution, including processes involving subglacial water. Finally, based on newly discovered insights, the impact of climate change on the stability of glaciers is discussed.

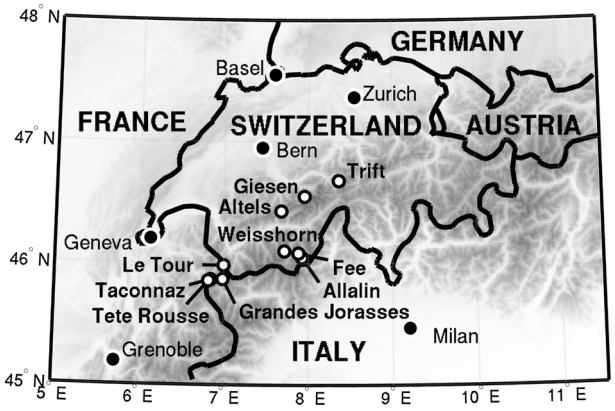

Figure 1. Geographical situation of the glaciers discussed in this study.

2. Classification of Avalanching Glacier Instabilities

Three types of avalanching glacier instabilities may be distinguished, depending on the thermal regime at the ice/bedrock interface and the presence of liquid water in the glacier. Hence, the distinction between balanced and unbalanced glaciers made by *Pralong and Funk* [2006] is not sufficient to distinguish between the different observed types of glacier instabilities. The thermal nature of the contact between the glacier and its bedrock plays a key role that needs to be taken into account in such a classification [*Röthlisberger*, 1981; *Alean*, 1985; *Huggel et al.*, 2004; *Faillettaz et al.*, 2011a, 2012]. As basal properties drive the nature of the instability, we propose the following distinction:

1. Glaciers that are entirely frozen to their bedrock (corresponding to cold glaciers according to *Pralong and Funk* [2006]), where the instability results from the progressive increase of internal damage due to the change in glacier geometry. In this case, the final rupture occurs within the ice, typically a few meters above the bedrock (section 3);
2. Glaciers that are partly frozen onto their bedrock with the presence of a temperate zone (corresponding to a transition state between a cold and temperate regime). In this case, the final rupture occurs directly on the bedrock in the temperate area and can possibly propagate through the ice. Contrary to the previous type of instability, liquid water is present in the glacier and plays a key role in the development of the instability. Although not flowing but locally trapped in the glacier, meltwater may contribute to the onset of a localized weakly adhering temperate zone at the interface between the glacier and its bedrock [*Faillettaz et al.*, 2011a] (section 4);
3. Temperate steep glacier tongues subject to sliding on their bedrock (corresponding to balanced glaciers according to *Pralong and Funk* [2006]). In this case, the final rupture occurs directly at the bedrock. Contrary to the previous type of instability, the glacier is sliding on its bedrock and flowing water is present at the interface between the glacier and the bedrock. The instability results mainly because of rapid changes in subglacial water runoff causing decoupling and recoupling glacier/bedrock processes (section 5).

In the following, each type of instability is analyzed on the basis of case studies. The results allow a better understanding of the processes leading to the final rupture and enable discussion of opportunities to predict an impending breaking off event.

3. Instabilities of Cold Glaciers

To illustrate the instability of unbalanced cold glaciers, i.e., the snow accumulation is mostly compensated with break off [*Pralong and Funk*, 2006], we shall first consider the Weisshorngletscher (Figure 1) as an example. This case is of particular interest as two events have been carefully monitored in 1973 and 2005 [*Flotron*, 1977; *Faillettaz et al.*, 2008], providing a unique opportunity for a better understanding of the evolution of the failure process leading to the break-off event. These results will be used to discuss the evolution of other unbalanced cold glaciers such as the Grandes Jorasses glacier.

3.1. Weisshorngletscher

The northeast face of the Weisshorn (Valais, Switzerland) is covered with unbalanced cold ramp glaciers located between 4500 and 3800 m above sea level (m asl), on a steep slope of 45 to 50° (Figure 2). The

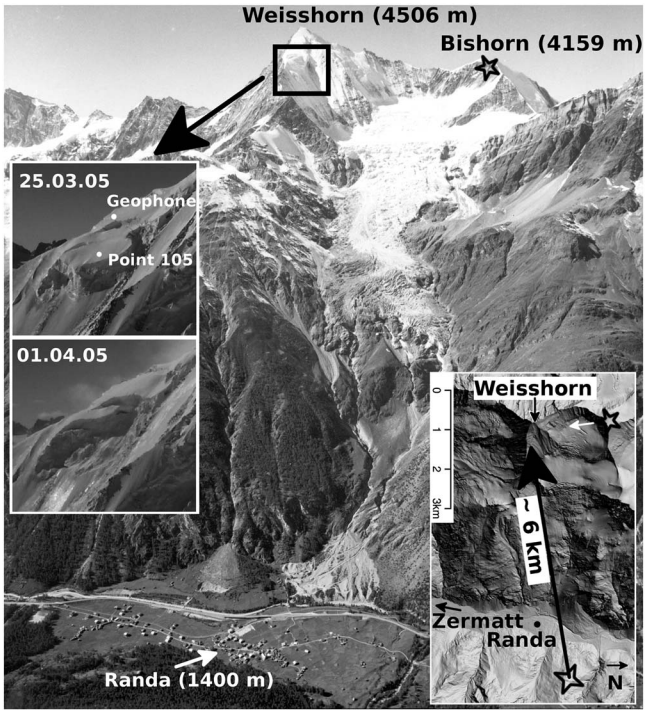

Figure 2. The east face of Weisshorn with the hanging glacier and the Mattertal with the village of Randa (photo: archiv VAW). The hanging glacier is marked with a circle. The left insets shows the hanging glacier on 25 March 2005 before the second break off (top) and on 1 April 2005 after the break off (bottom). The positions of the geophone and stake 105 used for displacement measurements are also shown. The bottom right inset shows an aerial view of the Weisshorn hanging glacier, and the monitoring setting (theodolite: large white four-pointed star and automatic camera: small white five-pointed star).

Weisshorn hanging glacier has broken off 5 times in the last 35 years (1973, 1980, 1986, 1999, and 2005, see *Raymond et al.* [2003]).

3.1.1. Monitoring Results

Surface Displacements. An unstable ice mass of 0.5×10^6 m^3 was detected in summer 1972. *Flotron* [1977] and *Röthlisberger* [1981] monitored the unstable portions of the glacier by means of distance measurements and photogrammetry. To predict the failure time, *Flotron* [1977] proposed an *empirical* power law function to fit the time evolution of the surface velocity measurements,

$$v(t) = v_0 + a(t_c - t)^m, \tag{1}$$

where $v(t)$ is the velocity at time t, v_0 is a constant velocity, t_c is the critical time, and $m<0$ and a are the parameters characterizing the acceleration. Note that observations of various other heterogeneous materials prior to the final rupture reveal the same power law behavior for several control parameters, such as displacement, velocity, or acoustic emissions [*Voight*, 1989]. Examples of such critical behavior can be found in a wide range of nonlinear processes such as natural ruptures, e.g., rockfalls [*Amitrano et al.*, 2005], landslides [*Sornette et al.*, 2004], volcanic eruptions [*Voight*, 1988], and earthquakes [*Bufe and Varnes*, 1993; *Bowman et al.*, 1998; *Jaumé and Sykes*, 1999; *Sammis and Sornette*, 2002], but also in finance and population dynamics [*Johansen and Sornette*, 2001]. By fitting data recorded over 250 days to equation (1), *Flotron* [1977] obtained a critical time t_c (time at which fitted velocity is infinite) at day 322, 2 weeks after the observed 1973 break off which occurred at monitoring day $t_f = 306$ day. The ice volume was a third of that expected as the glacier experienced a series of disaggregations resulting in many small break-off events.

In the following years, a progressive buildup of the hanging glacier was observed. Frontal crevasses had been perceptible since 2000, indicating a separation of the frontal part of the glacier. In 2005, the geometry of the glacier appeared to be almost identical to its geometry in 1973 before the catastrophic event, suggesting an imminent rupture. In the same way as in 1973, surface displacements were carefully monitored on different points of the glacier 1 month before the final break off but with a greater accuracy (of about 1 cm)

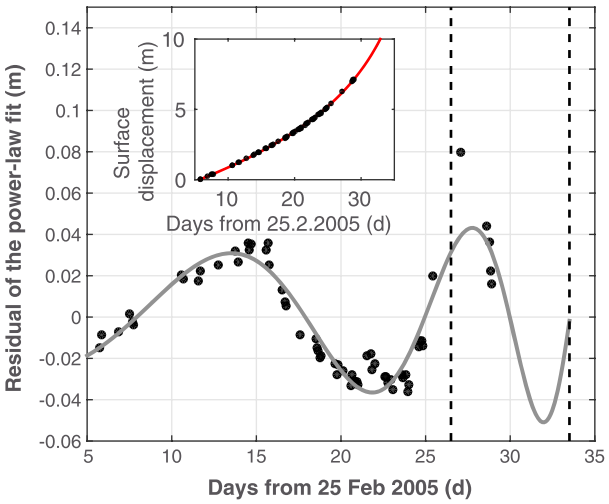

Figure 3. Residual of the power law fit of the surface displacement records illustrating the oscillating behavior. The two vertical dashed lines indicate the observed two successive break-off events (after 26.5 and 33.5 days of monitoring). (inset) Surface displacements with the corresponding power law fit (in red). Reprinted from the Journal of Glaciology with permission of the International Glaciological Society.

[*Faillettaz et al.*, 2008]. Derived surface velocities show two distinct zones: an upper one with nearly constant velocities and a lower one with increasing velocities. The zone with nearly constant and small surface velocities did not break off, whereas the other experienced a rupture. Analyzing surface velocity at different locations could help to estimate the volume of the unstable ice mass. Surface displacements before the 2005 break off showed a similar behavior as before the 1973 instability, indicating a power law acceleration before the catastrophic rupture. Moreover, due to the high accuracy of the surface displacement measurements, log-periodic oscillations superimposed on this acceleration (see section 3.1.2 for appearance and interpretation) could be detected [*Pralong et al.*, 2005; *Faillettaz et al.*, 2008] (Figure 3). The time evolution of the surface displacement measurements can be described with the following equation [after *Sornette and Sammis*, 1995; *Pralong et al.*, 2005]:

$$s(t) = s_0 + u_s t - a(t_c - t)^m \left[1 + C \sin\left(2\pi \frac{\ln(t_c - t)}{\ln(\lambda)} + D\right)\right], \quad (2)$$

where $u_s t$ is a continuous displacement, t_c the critical time, $m < 1$ the power law exponent, a a constant, C the relative amplitude, λ the logarithmic frequency, and D the phase shift of the log-periodic oscillation.

Faillettaz et al. [2008] also demonstrate that the log-periodic fit is more robust and yields more accurate results on the time of failure than a simple power law fit. Using a Lomb periodogram analysis [*Press*, 1996; *Zhou and Sornette*, 2002a], which is designed to analyze nonuniformly sampled time series, two log frequencies could be identified, corresponding to $\lambda_1 = 1.93$ and $\lambda_2 = 4.2$, with $\lambda_2 \approx 2\ \lambda_1$. The value and the existence of such subharmonic log frequencies have important implications on the physical interpretation of the rupture process leading to the final rupture (see section 3.1.2). However, such an analysis is only possible if topographic measurements of surface displacements are accurate enough (i.e., 5 mm). Alternatively, recording the icequake activity before the final rupture is expected to describe the crack (or damage) evolution within the ice mass during the failure process and also possibly provide new insights on the physical processes leading to the final rupture. Note also that, like GPS measurements, this monitoring system is working under all weather conditions.

Seismic Analysis. The fracturing of brittle heterogeneous materials has often been studied using seismic emission measurements (see, for instance, *Johansen and Sornette* [2000] and *Nechad et al.* [2005a, 2005b] for recent observations interpreted using concepts relevant to the present study). Tools to record seismic emission have already been used at the mesoscale to find precursors to natural gravity-driven instabilities such as cliff collapse [*Amitrano et al.*, 2005] or slope instabilities [*Dixon and Spriggs*, 2007; *Kolesnikov et al.*, 2003; *Dixon et al.*, 2003]. The present section focuses on the seismic emissions generated by a hanging glacier before its breaking off.

Several studies have shown that glaciers can generate seismic signals called icequakes [*Neave and Savage*, 1970; *Röthlisberger*, 1955]. Previous studies have identified at least five characteristic seismic waveforms associated with five different types of icequake events.

These include (1) brittle deformation of ice induced by surface crevassing [*Neave and Savage*, 1970; *Deichmann et al.*, 2000; *Walter et al.*, 2008], (2) basal sliding [*Weaver and Malone*, 1979; *Ekström et al.*, 2003,

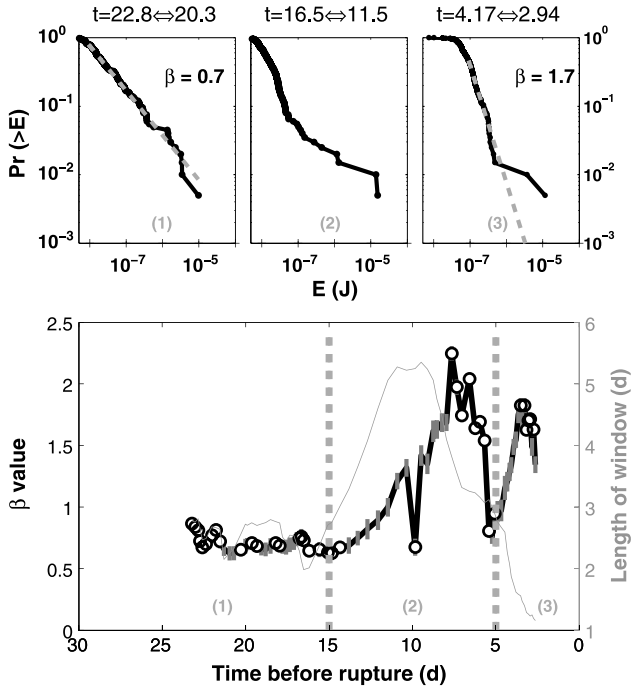

Figure 4. (top) The three plots show the complementary cumulative size-frequency distribution (CSFD) ($Pr(> E)$) of icequake energies (E) obtained in three windows of 200 events each, ending at the time indicated in the panels. (bottom) The evolution of the exponent β of the power law fitting the CSFD obtained in running windows of 200 events. The exponent β has been estimated using the maximum likelihood method. The thin gray line also gives the duration of the sliding window of 200 events, corresponding to the scale on the right. The vertical lines indicate the errors given by the maximum likelihood method. The maximum likelihood fitting method with goodness-of-fit tests based on the Smirnov test [*Clauset et al.*, 2009]. Empty symbols indicate those fits for which the power law behavior is plausible. The vertical gray dotted lines indicate the transition between the different regimes (i–iii) (see text). Reprinted from the Journal of Glaciology with permission of the International Glaciological Society.

2006], (3) hydraulic transients in intraglacial water channels [*St. Lawrence and Qamar*, 1979; *West et al.*, 2010], (4) calving events [*Qamar*, 1988; *O'Neel et al.*, 2007; *Amundson et al.*, 2008; *Nettles et al.*, 2008; *Walter et al.*, 2010, 2012], (5) iceberg interaction [*MacAyeal et al.*, 2008], and (6) stick-slip motion [*Wiens et al.*, 2008; *Winberry et al.*, 2013; *Allstadt and Malone*, 2014].

During the 25 day period of seismic monitoring at Weisshorngletscher, *Faillettaz et al.* [2011b] identified a total number of 1731 icequakes and calculated their corresponding energy. Seismic events with short and impulsive signals and similar spectra were observed, with dominant power contained in the 10–30 Hz frequency band, which is consistent with previous on-ice seismic recordings [*Neave and Savage*, 1970; *Deichmann et al.*, 2000; *O'Neel et al.*, 2007; *Roux et al.*, 2008]. This frequency band was associated with fracture growth prior to a calving event [*O'Neel et al.*, 2007] for water-terminating glaciers. In these cases lower frequency signals between 1 and 3 Hz were also observed, but the generation of these signals most likely involves liquid water [*O'Neel and Pfeffer*, 2007; *Bartholomaus et al.*, 2012]. This would explain why they are not observed in the case of the hanging glacier at Weisshorn.

Faillettaz et al. [2011b] characterized the evolution of the seismic activity by using two different metrics based on the icequake energies (Figure 4) and the waiting times between two events (Figure 5). They evaluated the time evolution of the complementary cumulative size-frequency (also called "survival") distribution (CSFD) of the icequake energy prior to the break-off event using a moving window of 200 events with a 20-event shift (Figure 4).

Three different successive behaviors were observed (Figure 4): (i) for the windows located close to the start of the measurements (up to $t \simeq 14$ day before the break off, time being measured backward with $t = 0$ at the event), the CSFD corresponds to a power law distribution over at least 3 orders of magnitude, indicating a scale invariance of the seismic emissions; (ii) from $t \simeq 14$ day to $t \simeq 5$ day before the break off, the CSFD no

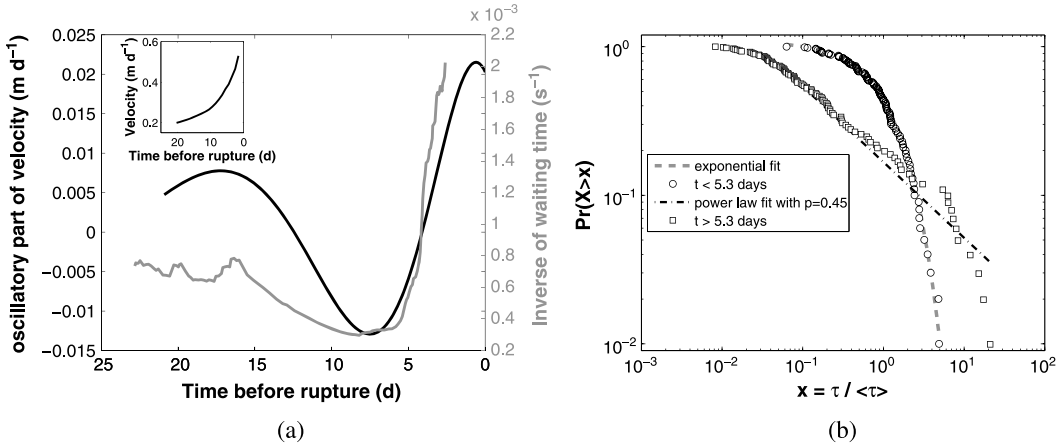

Figure 5. (a) Plot of the inverse of the waiting time between successive icequakes (noisy grey curve) and of the oscillatory part of the evolution of the surface velocity (smooth dark oscillatory curve). (inset) Surface velocity as a function of time up to the first break off. (b) Complementary waiting time distribution ($Pr(X > x)$) for the 100 events before and after the transition between stable and unstable regimes ($\simeq$ 5.3 days). The waiting time between two icequakes is τ, and $\langle\tau\rangle$ is the mean of all the waiting times considered. The data for $t \leq 5.3$ days can be well fitted by the exponential function $p(x) \sim a \cdot \exp(bx)$ with $a = 110$ and $b = -0.93$. For $t \geq 5.3$ days, the distribution of waiting times was compatible with a power law $p(x) \sim x^{-\alpha}$ for $x > x_{\min}$ with $\alpha = 1.5$ and $x_{\min} = 0.058$. Reprinted from the Journal of Glaciology with permission of the International Glaciological Society.

longer follows a power law, suggesting a change in the damage evolution process developing in the ice mass; (iii) for the time windows close to the end of our observational period (after $t \simeq 5$ day before the break off), the CSFD recovered a power law behavior, with a high power law exponent value.

Moreover, performing the same statistical analysis for the waiting time between two icequakes, *Faillettaz et al.* [2011b] also observed a change in the waiting time distribution occurring about 1 week before the final rupture. It appears that (i) the waiting time distribution between successive icequakes is initially well described by a power law distribution, indicating a temporal correlation between the icequakes; (ii) 5 days before the rupture, the waiting time distribution became exponential, indicating a loss of temporal correlation between the icequakes (Figure 5b).

3.1.2. Interpretations and Discussions

Appearance of Log-Periodic Oscillations of Surface Displacements. It was suggested in section 3.1.1 that the time evolution of the surface displacement measurements follows a log-periodic behavior (equation (2)). In general, the appearance of such log-periodic behavior results from a Discrete Scale Invariance (DSI)—which is a weaker kind of scale invariance according to which the system obeys scale invariance only for a specific scaling factor λ [*Sornette and Sammis*, 1995; *Sornette*, 1998; *Zhou and Sornette*, 2002b; *Sornette*, 2006]. DSI is thus a partial breaking of a continuous symmetry. The signature of DSI is the presence of power law with a complex exponent which manifests itself in the data by the appearance of log-periodic oscillations superimposed on a power law [*Sornette*, 2006]. Different physical processes were put forward to explain this behavior:

1. Several attempts have been made to link log-periodic oscillations to a system that contains a relaxation mechanism reducing the damage [*Ide and Sornette*, 2002]. However, the existence of such a relaxation mechanism in ice (negative feedback such as healing) is rather uncertain at such small time scales.
2. The evolution of damage anisotropy in the case of a shearing fracture was proposed by *Pralong* [2006] and *Pralong et al.* [2006] as a possible explanation for such an oscillating behavior. The existence of log-periodic oscillations emerges naturally from the classic constitutive equations of anisotropic damage evolution and ice deformation in the case of shearing flow.
3. The appearance of the log-periodic oscillations could also result from dynamic crack interaction, as shown by *Huang et al.* [1997] and *Sahimi and Arbabi* [1996]. A possible physical interpretation could be that small cracks develop in a shear band close to the glacier bed, because of large strain rates. As a result of fracture mechanics, the largest cracks will be less screened and will thus grow faster, eventually stopping the smaller cracks. *Huang et al.* [1997] showed that, for the growth of a population of cracks oriented in one direction,

this mechanism leads to a spontaneous generation of discrete scale invariance with a preferred scale of $\lambda = 2$. Moreover, subharmonic frequencies appear naturally and are arbitrary powers λ^n of the preferred scaling ratio λ which corresponds exactly to what was found in section 3.1.1 with the Lomb periodogram analysis.

Different plausible physical mechanisms are able to produce the observed log-periodic oscillating behavior of the surface displacement measurements. All are associated with a partial breaking of continuous symmetry. In this context, the dominant mechanism present during destabilization seems to be the dynamic crack interaction, as it provides an additional framework to explain the concomitant observed seismic activity (see below).

Seismic Activity. Faillettaz et al. [2011b] also analyzed the seismic activity radiating from the glacier before its break off (see Figure 4). Their results clearly indicate three regimes: (i) up to 2 weeks before the break-off event, the seismic activity was relatively stable; (ii) then the seismic activity decreased; and finally (iii) around 1 week prior to the break-off event, the seismic activity drastically increased (Figure 5a). The same results were observed experimentally in heterogeneous materials, in agreement with a power law divergence expected from the critical point theory [*Johansen and Sornette*, 2000], where rupture is considered as a phase transition resulting from the collective organization of defects that interact to prepare the global transition (i.e., the rupture) [*Sornette and Sornette*, 1990; *Sornette and Vanneste*, 1992; *Anifrani et al.*, 1995; *Andersen et al.*, 1997; *Sornette and Andersen*, 1998; *Sammis and Sornette*, 2002].

Moreover, *Faillettaz et al.* [2011b] were able to show a clear correlation between icequake activity and the oscillatory part of the velocity, suggesting that the seismic activity is not correlated with the global power law acceleration but rather with the jerky motion events superimposed on the overall accelerations (see Figure 5a). Crack coalescence (see section 3.1.2) is a possible explanation for this change in the distribution of waiting times from power law to exponential behavior (Figure 5b). The random activation of different damage clusters when approaching the global failure causes a transient loss of the temporal correlation of the individual fracture events [*Kuksenko et al.*, 2005]. This effect confirms the existence of a hierarchical structure in the fracture process in the glacier. *Faillettaz et al.* [2011b] attributed this change of behavior to the transition from a diffuse to a cluster damage organization.

Synthesis of the Failure Evolution Leading to the Break Off. Combining all results (see Figure 6), the following sequence of failure processes leading to the final break off could be evidenced:

1. An initial, stable phase related to a self-organizing regime, where diffuse damage accumulates within the glacier, with a proliferation of dislocation-like defects. In other words, the glacier has time to adapt to the deformation rates and to the damage maturation process.
2. A transitional phase where the damage process proceeds, microcracks grow and start merging in a homogeneous way. Log-periodic oscillations appear and reveal the hierarchical structure of the fracture process under development.
3. A catastrophic regime where damage clusters are randomly activated. Damage clusters interact and merge with a preferential direction (i.e., preparing the final rupture pattern), in contrast to the previous regime. The largest scale of the hierarchical structure of the fracture process is activated (resulting in characteristic events).

Based on this behavior, both seismic and surface displacement precursory signals of the imminent catastrophic rupture could be identified (red arrows in Figure 6), such as the appearance of log-periodic oscillations in the surface displacements, an evolution in seismic activity, changes in the icequake size-frequency distribution and in the waiting time distribution.

These results provide new insights into the possibility of a real-time diagnostic of the stability of a hanging glacier with the help of seismic monitoring. Such a real-time diagnostic is based on these precursory signs: (i) the change of power law exponent of the CSFD related to the icequake energy, (ii) the transition from power law to exponential behavior in the CSFD of waiting times between icequakes, and (iii) the increase in seismic activity before the break off. A monitoring strategy could take advantage of the appearance of these different precursory signs before rupture, and by detecting and evaluating them, providing an estimation of the current stability (or imminence of a break-off event) should be possible in real time. Different attempts were undertaken recently with seismometers installed in the vicinity of the glacier [*Dalban Canassy et al.*, 2012] (section 5.2) or directly on ice [*Dalban Canassy et al.*, 2013].

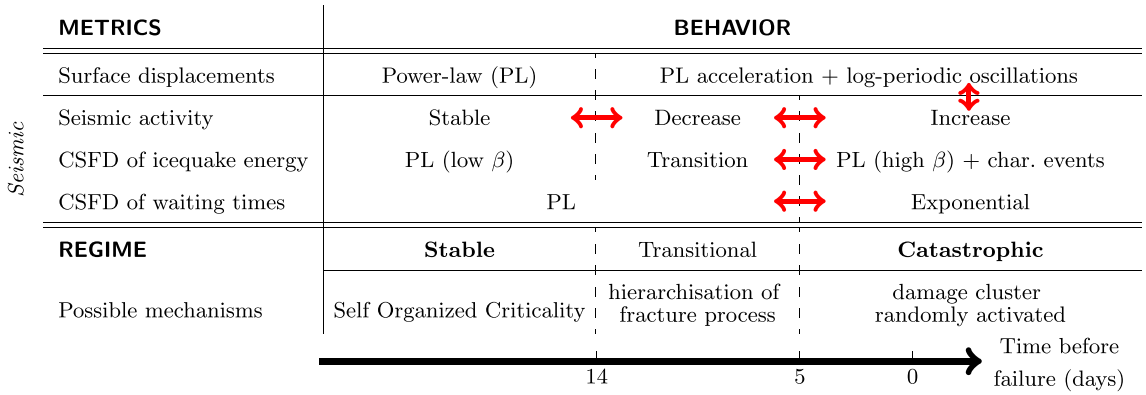

Figure 6. Summary of the evolution of different behaviors associated with the different metrics (CSFD, see text) as a function of time. Red arrows indicate the possible precursors to the break-off event. The origin of time 0 corresponds to the occurrence of the first break-off event on 24 March 2005 (after 26.5 days of monitoring) with an estimated volume of about 120, 000 m^3.

3.2. Application to the Grandes Jorasses Glacier

The results and methods obtained on the Weisshorn hanging glacier were applied to the case of another unbalanced cold glacier located on the south face of Grandes Jorasses. The Grandes Jorasses glacier (Figure 1) is located at an elevation of 3950 m asl (Figure 7) above the Italian Val Ferret, a famous and highly frequented touristic site both in winter and summer. Historical data and morphological evidence indicates that the glacier is subject to recurrent icefalls which can be dangerous, particularly in winter, as they can trigger catastrophic combined snow and ice avalanches. The last major break-off event with an ice volume estimated to 150, 000 m^3 reaching the bottom of the valley (Figure 7) occurred without damage in June 1998. In the following years, the hanging glacier has progressively reformed and has almost recovered its critical geometry of 1998 (Figure 7), and a monitoring program was initiated. It consisted of surface displacement measurements (with automatic total station and GPS, Figure 8), close-range photogrammetry (Figure 9) and seismic activity [*Margreth et al.*, 2011]. Unfortunately seismic monitoring failed due to instrument problems.

Surface displacements (Figure 8) were continuously measured at different stakes in the course of the year 2010 at 1 h intervals with the aim to timely detecting an impending ice fall [*Margreth et al.*, 2011]. Using the same correction technique as *Faillettaz et al.* [2008], surface displacement data could be evaluated with an accuracy

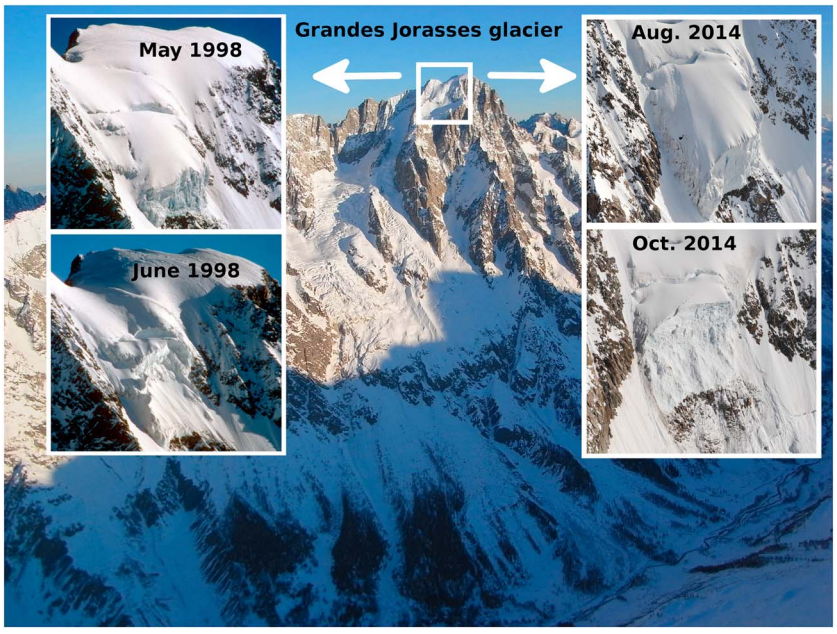

Figure 7. South side of the Grandes Jorasses and the Italian Val Ferret. (left inset) Evolution of the hanging glacier from May to June 1998. (right inset) Evolution of the hanging glacier from August to October 2014.

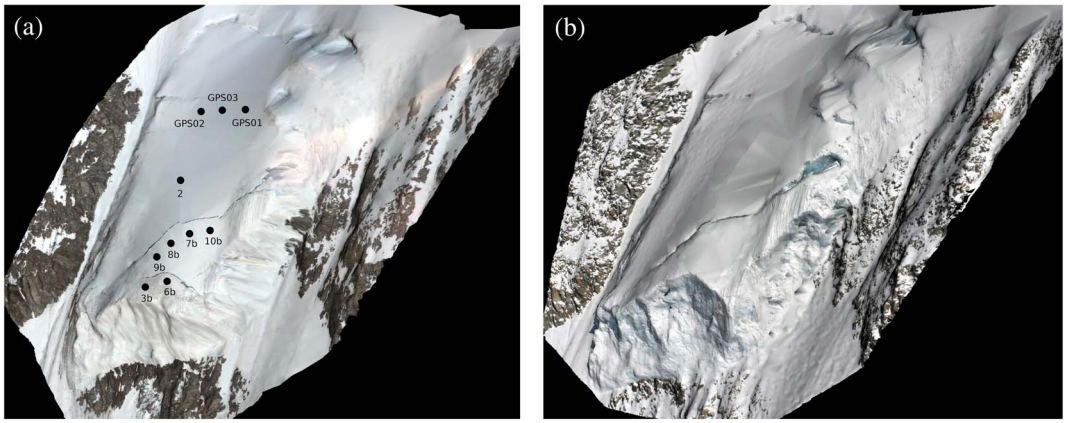

Figure 8. Grandes Jorasses hanging glacier (a) on 8 July 2010 and (b) on 31 July 2010 with the position of the reflectors (black dots). The opening of the medium crevasse as well as the ice fall are evidenced.

of around 1 cm and allowed to infer surface velocities. The values appear to be about 50% higher in summer than in winter, probably because of the higher water content in the firn/ice at depth. As already observed at the Weisshorn hanging glacier, the medium crevasse (Figure 8a) separates the glacier into two distinct zones with different behaviors: a relatively stagnant zone located above the crevasse and an active zone downstream with higher surface velocities. Moreover, the opening of the medium crevasse (Figure 8b) was detected in mid-July indicating a further decoupling of the lower unstable part of the glacier. The motion of the reflectors called "3b" and "6b" (see Figure 8a) started to accelerate in June 2010 and measurements stopped around 7 July. *Margreth et al.* [2011] showed that surface displacements exhibited a log-periodic power law acceleration in the same way as for the Weisshorngletscher. This acceleration of the two reflectors led to an alert to the authorities of an impeding ice fall, which finally occurred on 24 July.

During this period, a close-range photogrammetric analysis was performed. By comparing two DEMs within a 1 year time interval, a slight thickening of the glacier behind the front and thinning in the upper part are evidenced. This observation indicates a mass transfer toward the front (Figure 9). This may indicate a progressive damage evolution within the ice above the bedrock in the central part of the glacier, leading to a global destabilization of the glacier in the coming months/years as previously observed in 1998 and confirmed with a combined ice dynamic and damage evolution modeling study [*Pralong and Funk*, 2005].

Although the volume of the serac fall was very small (approximately 7000 m^3 based on the photogrammetric analysis), global behavior appears to be the same as for large events (e.g, Weisshorngletscher), confirming that a break-off event can be accurately predicted independently of its final volume in the case of cold

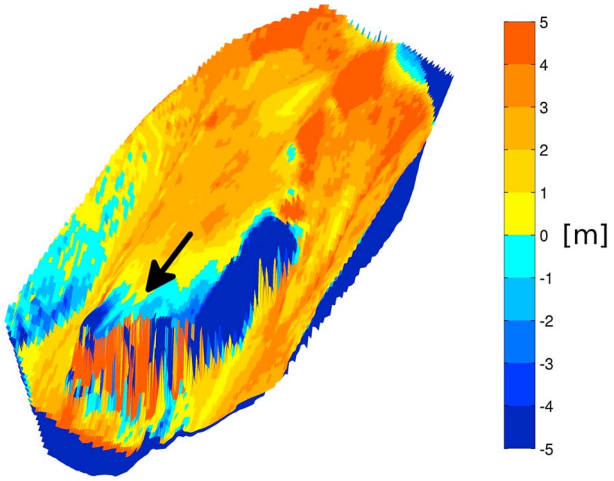

Figure 9. Comparison of two digital elevation models (DEMs) of the surface topographies in June 2009 and June 2010. In red where the glacier thickness decreased and blue where it increased.

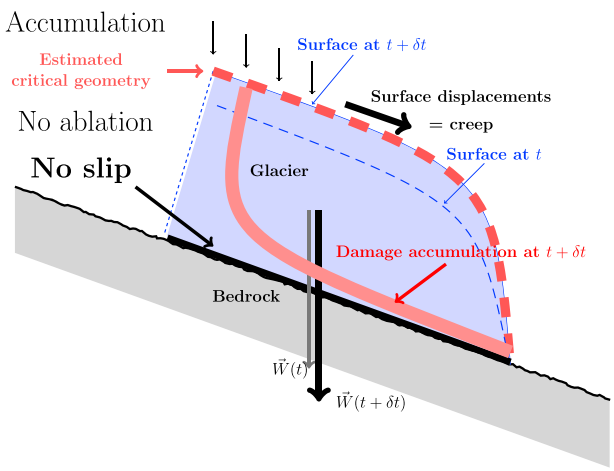

Figure 10. Schematic evolution of the instability in the case of an unbalanced glacier where *W* is the weight of the glacier. Damage accumulation refers to the increased density of microcracks within the cold glacier.

hanging glaciers, based on high-quality data of surface displacements. Moreover, depending on the location of the accelerating reflectors, a first guess on the final volume of the event could be achieved, as in the Weisshorngletscher case. Surface displacements were continuously surveyed since 2010. The Grandes Jorasses glacier finally broke off with an estimated ice volume of same order of magnitude as the 1999 event (about 150,000 m^3). Contrary to the 1999 event, it broke off in two events on 23 September and on 29 September 2014, without reaching the valley (Figure 7). Such a break off could be successfully anticipated based on the methods described in section 3.1.1, leading the authorities to secure the area a week in advance.

3.3. Conclusions Concerning Breaking Off of Cold Hanging Glaciers

Unbalanced cold glaciers periodically give rise to break-off events when their mass and ice thickness increases toward a critical geometry. Once their critical geometry is reached, the break off is inevitable. However, assessing the exact timing of the catastrophic event is problematic. The physical mechanisms at work during the destabilization are now better understood, thanks to the analysis of both seismic and surface displacement measurements: first, microcracks develop a few meters above the bedrock (see Figure 10). Then, after reaching a critical damage size, these microcracks start to merge (giving rise to log-periodic oscillations) and the previous stable regime shifts into a catastrophic one where the glacier has no time to adapt to the internal damage evolution. The catastrophic rupture is then inevitable. Precursory signs were found, principally based on seismic measurements. With a careful analysis of the rate of icequake generation, it was possible to detect the transition between these stable and unstable regimes and to assess the time of the final rupture. By combining the analysis of surface motion with log-periodic oscillations and icequake activity in the course of the rupture maturation process, the assessment of the time and the volume of the final break off can be significantly improved. The present study also provided new insights into the physical mechanisms of the rupture in heterogeneous materials.

4. Instability Due To a Rapid Transition From a Cold to a Temperate Glacier Bed

Altelsgletscher, 1895. In a recent study *Faillettaz et al.* [2011a] showed that a glacier instability could be initiated by a rapid localized warming at the glacier-bed interface leading to a weakening of the basal support. To illustrate such types of instability, we shall consider the gigantic break off of the Altelsglestcher as an example.

The Altels summit (Berner Oberland, Switzerland, Figure 1) is 3629 m asl high with a pyramidal shape. The northwestern flank is 1500 m high and 35° to 40° steep (Figure 11). In the middle of the nineteenth century, this face was largely covered with an unbalanced ramp cold glacier located between 3629 and 3000 m asl. In the early morning of 11 September 1895, a large part of this glacier broke off and gave rise to a huge ice avalanche. This catastrophic break off was carefully described and reported by *Heim* [1895], *Forel* [1895], *Du Pasquier* [1896], and later on by *Röthlisberger* [1981].

The volume of released ice was estimated at 4×10^6 m^3, which is the largest known icefall event in the Alps. The resulting ice avalanche caused the death of six people and 170 cows. Due to its huge velocity

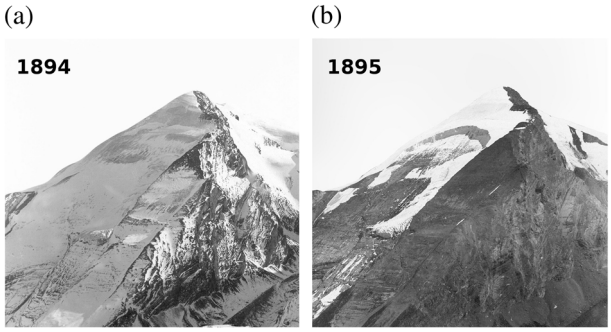

Figure 11. The Altelsgletscher (a) before and (b) after its break off (photograph P. Montandon, 25 November 1894 and 15 September 1895; Archive Alpine Museum, Bern).

[i.e., 430 km h^{-1} [*Heim*, 1895; *Röthlisberger*, 1981], this avalanche piled up 300 m on the opposite slope toward the Üschinengrat [*Faillettaz et al.*, 2011a]. An area of about 1 km^2 of the pasture was buried under a 3 to 5 m thick ice/debris layer. As *Forel* [1895] reported, a similar event had already occurred at the same place in 1782, killing four people and hundreds of domestic animals [*Raymond et al.*, 2003]. *Forel* [1895] pointed out that the summer 1895 was warmer than usual. Nowadays, this could not happen again because the Altelsgletscher has almost disappeared (a small tongue remains on its left side, which will melt away in the coming years).

Numerical Model Applied to the Altelsgletscher. To investigate the causes of this instability, *Faillettaz et al.* [2010] used a newly developed numerical model designed for describing natural gravity-driven instabilities. This model allows us to test the different hypotheses proposed previously and to explore the possible causes of the break off. A complete model description can be found in *Faillettaz et al.* [2010]. In a nutshell, the model takes into account the progressive maturation of a heterogeneous mass toward a gravity-driven instability, characterized by the competition between frictional sliding and tension cracking. The glacier is discretized into a regular two-dimensional array of ice blocks that can slide on the given bedrock topography. Each block interacts with its neighbors via elastic-brittle bonds. A realistic state- and rate-dependent friction law derived from *Ruina* [1983] and *Dieterich* [1994] was used for describing the block-bed interaction [*Faillettaz et al.*, 2011a]. The evolution of the inner material properties of the ice and its damage evolution eventually leading to failure were modeled by means of a stress corrosion law governing the rupture of the bond [*Nechad et al.*, 2005b]. In order to reproduce cracking and dynamic effects, the equations describing the motion of each block (including its inertia) are solved simultaneously. The details of this model, especially the friction and creep laws, are discussed in detail in *Faillettaz et al.* [2011a].

Numerical Results and Discussion. The main result of the different simulations performed on this glacier with the aim of reproducing the particular arch shape of the crown crevasse was a reduction of the basal friction coefficient in a limited area (Figure 12). One possible interpretation of the appearance of this weak zone is meltwater infiltration trapped within the cold ice of the glacier (Figure 12) [*Irvine-Fynn et al.*, 2011]. Climatic observations indicate that the air temperatures were higher than usual during the summer in the 3 years before the event and therewith support this interpretation.

Moreover, the simulations highlighted a two-step behavior: (i) a first quiescent phase, without visible changes with a duration depending on the rate of decrease of the friction coefficient, and (ii) an active regime with a rapid increase of basal motion during the few days before the break off. As a consequence, a crown crevasse opens only a few days prior to the rupture (which was suspected by A. Heim from the vague observations of local people). This means that the destabilization process of a hanging glacier due to a progressive warming at the ice/bed interface toward a partially temperate regime is expected to occur without visible signs until a few days prior to the collapse.

This result could be reinterpreted in the context of phase transition framework. The idea that there is a relation between fracture and phase transition is not new (for a review, see *Alava et al.* [2006]). In a nutshell, phase transitions are characterized by a change in the internal symmetries of a material as external control parameters are varied. In such a framework, fracture would be considered as a transition from an ordered phase to a disordered one. In general, two types of transition can occur: Either an abrupt "first-order" phase transition, with latent heat, coexistence, and no precursors, or a continuous "second"-order (or "critical") transition as time is

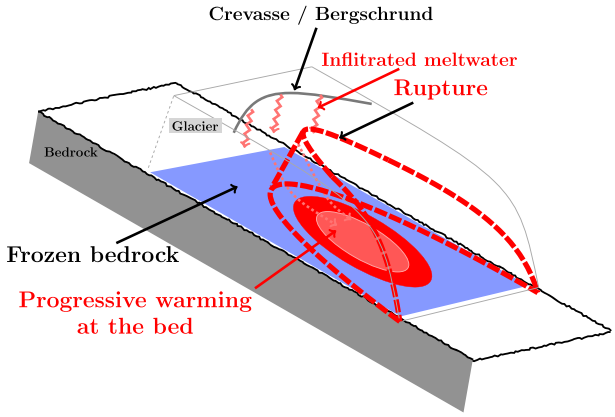

Figure 12. Schematic evolution of the instability initiated by a rapid localized warming at the ice-bedrock interface.

approaching the phase transition. Interestingly one can observe a first-order or a second-order transition in the same system, depending on the external conditions. In the critical point theory [*Johansen and Sornette*, 2000], rupture in heterogeneous materials is considered as a phase transition resulting from the collective organization of defects that interact to prepare the global transition (i.e., the rupture). In such a framework, rupture is considered as a second-order (critical) phase transition, where precursory signs announcing the final catastrophic break off exist. Cold glacier break-off events exhibit scale invariant behavior before rupture (surface displacement and icequake, section 3.1) that could be interpreted as a second-order phase transition. On the contrary, the "Altels instability" could be associated with a first-order phase transition where rupture appears abruptly, without precursory signs, as the *Griffith* [1921] theory of fracture in homogeneous materials. This difference in behavior can be explained by the varying time scale during each destabilization: during mechanical instabilities, damage develops in a quasi-static way and has time to interact and organize, resulting in a precursory seismic activity. On the contrary, the time scale of the Altels instability is rapid compared to the appearance of damage and its collective organization. The glacier has thus no time to adapt to the changes occurring at its ice/bed interface, explaining why the final catastrophic rupture occurs without precursors.

As a result, the only way to assess the stability of such a glacier is to detect in advance the progressive warming at the ice/bed interface (by measuring or/and modeling the evolution of the thermal regime of the glacier), or by trying to monitor trapped meltwater within the glacier. New promising field techniques based on Magnetic Nuclear Resonance were recently successfully used on the Glacier de Tête Roûsse (Chamonix, French Alps, Figure 1) to detect a subglacial water reservoir [*Vincent et al.*, 2012]. This technique seems to give reliable indications of the presence of water in a glacier but is a time-consuming work.

5. Instability of a Temperate Steep Glacier Tongue

5.1. The Allalingletscher

The problem of the instability of temperate steep glacier tongues is analyzed in the case of the Allalingletscher and the results are discussed in the context of other similar glaciers. The Allalingletscher was chosen because it broke off twice in the last century (i.e, in 1965 and 2000), and these events were well documented.

The Allalingletscher is located in the Swiss Alps (Valais, Switzerland, Figure 1) near the head of the Saas valley. Its tongue is temperate, and its altitude ranged from 2200 to 2800 m asl during most of the last century. The advance of its tongue repeatedly reached and blocked the river Saaser Vispa leading to the formation and the outburst of an ice-dammed lake until 1920 [*Röthlisberger and Kasser*, 1978].

5.1.1. The 1965 and 2000 Break-Off Events

The 1965 Break Off. On 30 August 1965, approximately 2×10^6 m^3 of ice broke off at the terminus of the Allalingletscher, moved down a rock slope of some 27° over the vertical distance of 400 m and continued for a farther 400 m across the flat bottom of the valley, claiming 88 victims at the Mattmark construction site. An overall view of the area shortly after the avalanche is shown in Figure 13.

Glaciological investigations showed that the ice avalanche has occurred during a phase of enhanced basal motion (termed "active phase") as a result of intensive bed slip of an even larger mass than the one that broke off on 30 August [*Röthlisberger and Kasser*, 1978]. Although it seemed that this particular condition was

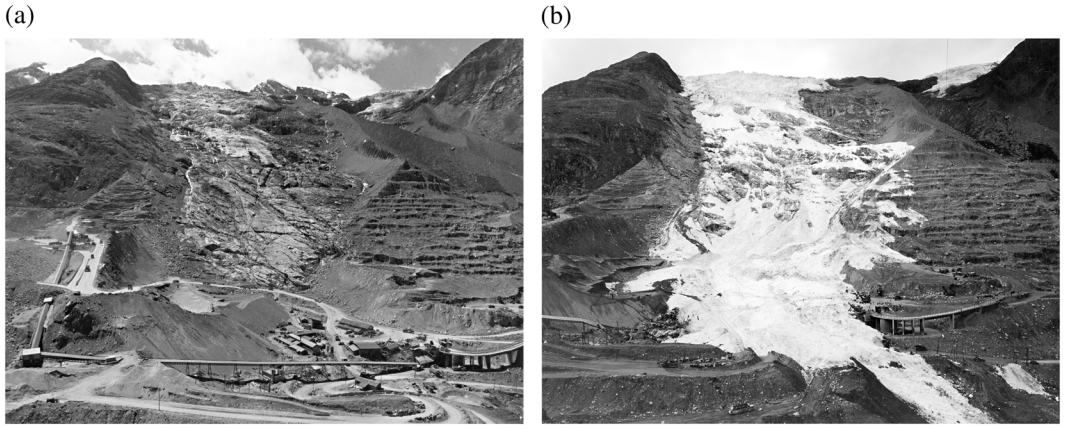

Figure 13. The Mattmark disaster: 2×10^6 m^3 of ice broke off on 30 August 1965 (archive VAW).

Figure 14. The Allalingletscher after the 1965 event (2×10^6 m^3 of ice on 30 August 1965) and after the 2000 event (1×10^6 m^3 on 31 July 2000) (photo archive VAW).

necessary for the lower part of the ice mass to slide off, it does not explain why the ice avalanche occurred in 1965 and not during other active phases reconstructed before and observed after this date. A certain topography of the bed, combined with an unfortunate mass distribution, was believed to have played a major role in the catastrophe.

The 2000 Break Off. In the year 2000, the glacier extent was similar to that of 1965. On 31 July, an ice volume of 1×10^6 m^3 broke off without causing any damage thanks to security measures (Figure 14). After this event, the position of the terminus continued to retreat, but at a very slow rate.

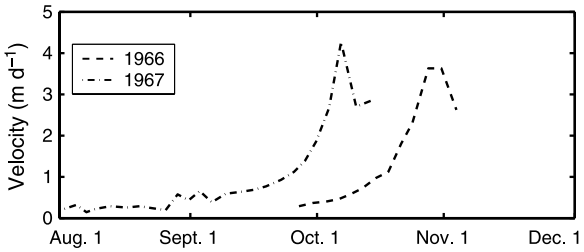

Figure 15. Surface velocities measured on the tongue of the Allalingletscher in 1966 and 1967. Archive VAW.

5.1.2. Data

After the 1965 break-off event a long-term monitoring program was initiated. It included, on a yearly basis, measurements of length change of the tongue, ice thickness changes along profiles, and Digital Elevation Models of the surface topography of the glacier tongue. Surface velocities were also measured at a subannual time scale in the 2 years following the break-off event.

The surface velocity measurements performed on the steep tongue after 1965 revealed periods with enhanced motion almost every year. These regular speedup periods can be well described with the power law acceleration already identified in the case of unbalanced glaciers (Figure 15). These "active phases" usually start in late summer and last for 2–3 weeks. *Röthlisberger and Kasser* [1978] pointed out a possible link with subglacial water flow (for a review, see *Irvine-Fynn et al.* [2011]). However, except for 1965 and 2000, these active phases ceased suddenly without triggering any major ice fall. Therefore, these active phases are not sufficient for the occurrence of a slide-off but are a necessary condition.

As shown by the length change data, the Allalingletscher readvanced rapidly after 1965 and recovered its previous geometry 5 years later. The glacier continued to advance up to 1984. Then, it started to retreat, and after 1997, at an accelerated rate.

The main results of the monitoring program carried out at the Allalingletscher obtained so far are the following:

1. Two major break off events occurred on 31 August 1965 and 31 July 2000.
2. The glacier tongue is *temperate*: the glacier is sliding on its bedrock (solid rock without debris).
3. A regular speedup of the glacier tongue lasting for 2–3 weeks has been observed almost every year after 1965 between July and October (called active phases).
4. Subglacial hydrology plays a major role in initiating and sustaining an active phase.
5. The active phase is only a *necessary condition* for the breaking off to occur.
6. A critical mass distribution within the glacier tongue is probably a key factor for the instability, because the observed two break-off events occurred when the glacier tongue reached a similar geometrical extension.
7. Contrary to the case of cold unbalanced glaciers, a break-off prediction based on surface velocity data is not possible.

5.1.3. Numerical Model Applied to the Allalingletscher

As it was recognized that an interaction between subglacial water flow and basal processes played a major role in the dynamical behavior of the steep tongue of the Allalingletscher, the model used in the case of Altels (section 4) was extended by including the effect of subglacial water flow [*Faillettaz et al.*, 2012] on the basal resistance [*Schweizer and Iken*, 1992; *Boulton et al.*, 2007; *Jay-Allemand et al.*, 2011; *Irvine-Fynn et al.*, 2011] where the friction coefficient is assumed to linearly decrease as subglacial water runoff increases. The extended version of the *Faillettaz et al.* [2010] model was used in the case of the Allalingletscher and applied to the geometrical extents of 1965 and 2000 (when a major part of the tongue broke off) and for the extent in 1984 (for the case where no significant ice fall occurred).

5.1.4. Results and Discussion

Modeling results confirmed the conclusions of a study by *Röthlisberger and Kasser* [1978]: (i) a critical geometrical configuration is required for a major destabilization of the glacier tongue, and (ii) active phases are triggered by an increase in subglacial water pressure. Moreover, our model results provided further insights into the maturation process of the instability: (iii) The subglacial drainage network has to be *distributed* over a major part of the tongue; (iv) the initiation of the fracturation process starts during the course of an activel

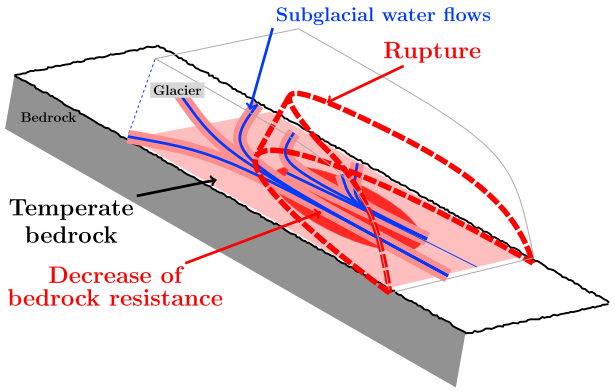

Figure 16. Schematic evolution of the instability for the case of a balanced glacier with a decreasing basal resistance due to increasing subglacial water pressure.

phase after a period of decreasing basal water pressure, i.e., during a phase of rapid recoupling of the glacier onto its bedrock. During this phase, an intensive fracturation of the ice is initiated. A catastrophic break off requires the combination of two opposing phenomena: first, the glacier needs to be in an active phase with strongly enhanced basal motion, and second, this active phase must be halted abruptly with a sudden recoupling of the glacier to its bed.

The plausibility of this process chain can be verified on the basis of observations during the years 2000 and 1965 when the glacier broke off. It appears that in both years, 1 month before the rupture, the meltwater input drastically increased leading to an active phase. During the 6 days prior to the break off, the runoff (assumed to be proportional to the meltwater input) dropped from 13 to 5 $m^3 s^{-1}$ in 2000 and from 14 to 5 $m^3 s^{-1}$ in 1965 [*Faillettaz et al.*, 2012]. Then the runoff started to increase again for a few days before the break off occurred. This suggests that once the glacier is recoupled onto its bedrock, an additional pulse of water is needed to trigger the instability. It appears that this observed sequence of basal water pressure changes corresponds to the process chain leading to the final break off identified with the modeling study.

This sequence of basal water pressure variations necessary to trigger the break off can be interpreted as follows: as the subglacial water channel stability is controlled by the balance between creep closure and melting of ice at the channel wall due to turbulent heat dissipation of the flowing water, a persistent runoff decrease would lead to a progressive channel closure and therefore to a reduction in the efficiency of the drainage network. A subsequent runoff pulse would inevitably lead to an increase in basal water pressure and corresponding decrease in basal resistance, which could possibly initiate the catastrophic break-off event (Figure 16).

5.2. Other Investigations

Similar Glacier Instabilities. Although rare, other similar instabilities have already been documented in detail (e.g., Le Tour 1949 [*Glaister*, 1951] and Feegletscher 2009 in *Faillettaz et al.* [2012]). Their careful analysis confirms that, as for the Allalingletscher, prerequisite conditions for a major destabilization were met and that an additional pulse in subglacial water was needed to trigger the final catastrophic event.

Monitoring Seismic Activity, the Triftgletscher (Bernese Alps, Switzerland). Recently *Dalban Canassy et al.* [2012] monitored the seismic activity of a steep glacier tongue at the Triftgletscher (Bernese Alps, Switzerland, Figure 1). The aim of this study was to investigate if seismic precursors of a break-off event could be detected in the case of a steep glacier tongue, as described in section 3 for the case of unstable cold glaciers. The glacier has experienced a rapid retreat during the last 20 years. After the year 2000, the tongue ended in steep terrain (about 35°) and its stability was questionable [*Dalban Canassy et al.*, 2011]. In the following summers, surface velocities increased from 1 to 4 m d^{-1}, similar to those observed at the Allalingletscher (Figure 15). However, up to now, no major break-off event has occurred. Such an event cannot be completely excluded, although a single water outlet stream was observed at the glacier terminus, suggesting a channelized rather than distributed subglacial water flow path (contrary to the Allalingletscher). This might be the reason why no substantial active phases have been observed so far at the Triftgletscher.

Results from seismic monitoring showed correlations between the seismic activity and subglacial runoff as well as possible signatures of stick-slip motion events. It seems that the phase of recoupling of the glacier to its bed could possibly be captured from peaks of released seismic energy ranging over several days or the detection of an event with large seismic energy generation. Further investigations are needed, however, to confirm the appropriateness of these seismic signals as precursory signs of a large-scale instability.

5.3. Summary

Glacier sliding instabilities may occur on steep temperate glacier tongues. Such instabilities are strongly affected by subglacial hydrology: infiltrated meltwater may indeed cause a lubrication of the bed and a decrease in the effective pressure at the glacier bed and consequently a decrease in basal friction. The three case studies presented here indicate that five different criteria have to be met for an instability to occur:

1. A critical geometrical configuration of the glacier tongue is needed (steep slope, no frontal abutment, and convex shape of bed topography).
2. The glacier should have experienced an active phase.
3. The subglacial drainage network has to be distributed.
4. A period of decreasing runoff is needed to reduce the efficiency of the drainage network and favored fracturation process.
5. Finally, a pulse of subglacial water flow is a likely trigger for the catastrophic break-off event.

Although promising, seismic survey is not yet developed enough to be used as a warning tool of impending large-scale break-off events [*Dalban Canassy et al.*, 2012] and no other appropriate surveying technique has been identified so far.

6. Climatic Changes and Glacier Instabilities

In the more general context, climate warming will likely affect the stability of some glaciers in the near future. Because of the ongoing glacier retreat, presently dangerous glaciers will disappear (e.g., Allalingletscher and Altelsgletscher), and in other cases glaciers may become unstable. To illustrate this evolution, an example of both cold and a partly temperate newly formed glacier instability is discussed below.

6.1. The Giesengletscher

As general glacier retreat in the Alps is observed, some glaciers could evolve to a critical geometrical extent. As an example, the Giesengletscher in Switzerland could be a suitable candidate to a future catastrophic break off. The terminus of the Giesengletscher is located at about 2500 m asl in the Bernese Alps (Figure 17). In 2008, a crevasse spanning the whole glacier width was observed on the glacier tongue, indicating an ongoing active phase on its steepest section (about 35°, Figure 17). The situation is nevertheless not critical yet, as the glacier terminus is resting on a moderately steep bedrock, which still stabilizes the glacier tongue (green zone in Figure 17). Moreover, its bedrock topography likely allows a distributed drainage network. Except for the stabilizing presence of the glacier terminus, all conditions for the glacier to break off are fulfilled, indicating that a retreat from the presently still-supporting terminus location could lead to a critical situation.

6.2. Glacier de Taconnaz: Warming at the Bedrock

The Taconnaz glacier (Figure 18) is a hanging glacier in the Mont Blanc area with an upper accumulation area of about 2 km^2 stretching down from Dôme du Goûter (4300 m asl). Along its way, the ice flow concentrates and a large part of the accumulated ice is channeled over an approximately 600 m wide ice cliff at about 3300 m asl. In this way, most of the ice accumulated upstream periodically breaks off. During winter, when the snow mantle is unstable, huge blocks of ice breaking off the cliff can trigger large avalanches made up of a mixture of snow and ice, representing a serious risk to inhabited areas below. The avalanches of 16 April 1984 and 20 March 1988 devastated a part of the village of Le Nant without victims. Large avalanche protection dams were built between 1985 and 1991 to protect the inhabitants. However, a large avalanche of snow and ice on 11 February 1999 at 4:30 A.M. overran the dam and stopped on a ski run, very close to the inhabited areas. Fortunately, nobody was in this area at the time. The volume of the 1999 avalanche was assessed to be about 750,000 m^3. In order to assess the volume and frequency of large ice collapses from the hanging glacier, numerous topographic and photogrammetric measurements have been performed to determine length and volume changes [*Le Meur and Vincent*, 2006; *Vincent et al.*, 2015]. From these observations, these authors have pointed out several major collapses that occurred once the cliff edge reached a threshold position. It seems that this threshold position has not changed over the last decade. In addition, they found that large break offs

Figure 17. The Giesengletscher in 2011 (archive VAW). The green zone indicates the stable part of the tongue and in red the likely unstable zone.

occur cyclically with a characteristic period of 6 months as the glacier recovers its critical geometry [*Le Meur and Vincent*, 2006; *Vincent et al.*, 2015]. It seems that this critical geometry is a necessary but not sufficient condition for large break offs. Indeed, in some cases, although the cliff edge reached the threshold position, the seracs disintegrated into small ice blocks without a large break off. A precursory sign that can be used to assess the instability of this hanging glacier could therefore be geometry changes at the ice cliff; however, this is probably not sufficient.

In addition, another issue concerning this glacier is related to its thermal regime. Indeed, the stability of this hanging glacier may be affected in the near future by changes in the thermal regime at the ice/bedrock interface. The first deep englacial temperature measurements in this region were performed in boreholes drilled into the glacier at Col du Dôme (4250 m asl) in 1994, 2005, and 2009. The temperature profiles obtained clearly indicate recent atmospheric warming. Results from a heat transfer model have revealed that englacial temperatures have increased due to rising air temperatures and latent heat produced by surface meltwater refreezing within the glacier [*Vincent et al.*, 2007; *Gilbert and Vincent*, 2013]. Depending on surface melt and snow accumulation, *Gilbert and Vincent* [2013] observed a temperature increase of 0.4°C and 1.2°C over the last decade at 40 m depth. In 2008, englacial temperature measurements performed at 3415 m asl on Taconnaz glacier, 150 m upstream of the ice cliff, indicated a basal temperature of −2.6 °C, which is not far from the melting point [*Vincent et al.*, 2015]. In addition, the englacial temperatures measured in the top 25 m of the glacier reveal temperate conditions. The situation can be compared to the case of the Altelsgletscher (section 4): The Taconnaz glacier is a cold hanging glacier, with a cold tongue cut by the ice cliff. Because of the high ice velocities at its terminus (more than 100 m a^{-1}, *Le Meur and Vincent* [2006]), the thermal regime there is likely dominated by the advection of cold ice from above. A progressive warming of the ice is expected to occur upstream and propagate downstream. At the same time, the glacier front is cooled by heat

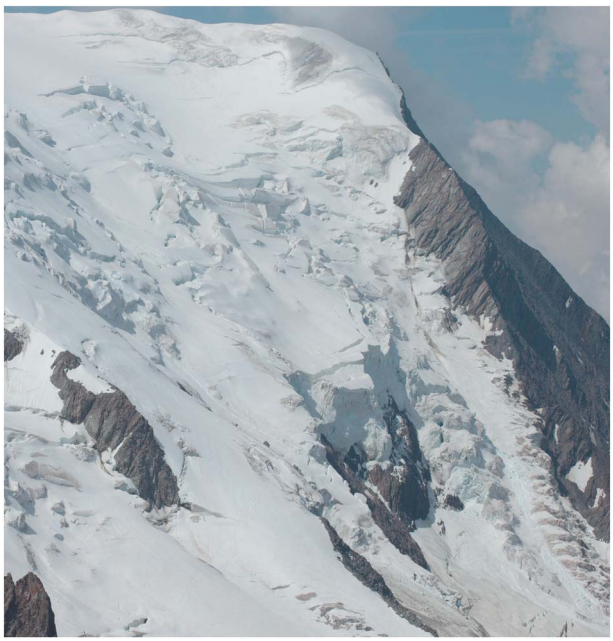

Figure 18. The Taconnaz glacier in 2012 (photo C. Vincent).

conduction through the frontal ice cliff and supporting rock wall (facing north), although this conduction is likely low due to the fast ice flow in this region (Mont Blanc, France). Additional deep ice temperature measurements in a borehole, performed in 2012 at the same location upstream of the ice cliff, revealed no change between 2008 and 2012 [*Vincent et al.*, 2015]. This suggests that the ice advection process is likely predominant in driving the ice temperature changes in this region over a period of a few years to a decade. It confirms that numerical modeling including heat transfer and ice flow modeling are required to assess the different heat source contributions and accurately simulate the ice temperature changes in this fast glacier [*Gilbert et al.*, 2014]. If sufficient meltwater is produced at the surface, it may be trapped at the ice/bed interface or within crevasses because of cold temperatures immediately behind the front. Successive hot summers could potentially warm the still frozen ice/bedrock interface, resulting in a reduction of the basal support. This could affect the stability of a major part of the glacier as already discussed for the Altelsgletscher. Detecting the transition from cold to temperate bedrock either by experimental or by numerical studies is the only way to assess glacier stability in this case. Application of the numerical model described in section 4 to this particular case could also help in assessing the effect of a growing temperate zone at the ice/bedrock interface and the size of the unstable zone.

7. Conclusions

Three types of glacier instabilities were identified according to the thermal properties at the ice/bedrock interface. If cold, the glacier is frozen to its bedrock and the final rupture propagates within the ice a few meters above the ice/bedrock interface. The maturation of the rupture is associated with precursory signs which can be used to predict the final break off. Two surveying techniques can be deployed for achieving such a prediction: (i) surface displacement measurements exhibiting a power law acceleration with log-periodic oscillations. By fitting the data to a corresponding function, a time prediction of the final break off might be possible. (ii) Moreover, monitoring the seismic activity generated by the glacier before its break off helps to better understand the processes leading to the final instability. The glacier destabilization can be divided into three regimes, each associated with specific precursory signs. In a first phase (i.e., a stable regime), damage appears progressively in the glacier. In such a regime the glacier has time to adapt to its internal changes. Then, in a transition regime, the microcracks reach a critical density where they start to interact and merge, leading to the observed log-periodic oscillations. Finally, in a catastrophic regime, these cracks merge into large damage clusters in a preferential direction (i.e., the final crack path). Combining the surface displacement and seismic survey provides new perspectives for an accurate breaking-off time prediction and real-time diagnostic of the glacier stability.

In the other types of glacier instability, water plays a key role in the initiation and the development of the instability. The presence of water greatly complicates the glacier behavior. If the ice/bedrock interface is partly temperate, the instability could be explained by the presence of meltwater trapped within the glacier that affects the extension of the temperate zone by release of latent energy produced when water freezes. The presence of meltwater at the ice/bedrock interface also reduces the basal resistance, promoting the onset of the instability. It can be shown that the resulting instability occurs without clear precursory signs. In such a case, the only way to detect the initiation of the instability is to monitor the time and extent evolution of the temperate zone at the interface.

The third type of instability concerns steep temperate glacier tongues. In such a case, the glacier slides off at the bedrock in the course of an active phase. Such events are always observed in late summer indicating that subglacial water flow plays a key role in triggering the instability. Prerequisite conditions required for the final break-off event to occur were identified. (i) The geometrical extent of the glacier has a major impact on the instability. If the glacier tongue rests on a steep slope and is affected by active phases, it may be subject to a major instability if the frontal abutment fails. (ii) The subglacial drainage network plays a major role in the instability. A pulse of subglacial water flow may lead to a sudden increase in water pressure and reduce basal resistance. If the drainage network is channelized, only a limited glacier area will be affected by subglacial pressure fluctuations reducing the likelihood of an instability. Conversely, a distributed drainage network will affect a major part of the glacier tongue. Numerical modeling confirmed that a distributed drainage network is mandatory for initiating an active phase. But it needs to be pointed out that a typical sequence of abruptly decreasing subglacial runoff followed by a water pulse is mandatory for triggering the break off. It appears that the so far observed break-off events occurred after a short period of reduced subglacial runoff. During this phase, the glacier is subject to an enhanced fracturation process due to its recoupling to the bed. Moreover,

during this period, the efficiency of the subglacial drainage network will be reduced so that a subsequent water pulse will reduce the effective pressure and facilitate the break off. Although the prediction of such an event remains far from being achievable yet, there is some hope to capture seismically the phase of enhanced fracturation process due to recoupling of the glacier to its bed and thus detect the potential unstable state of glacier.

In the more general context of climate change, the stability of some glaciers may be affected in the near future due to changes in thermal regime at the ice/bedrock interface or due to changes in geometrical extension. Although some presently hazardous glaciers will become harmless in the near future because of their retreat, others may evolve toward a critical situation and become dangerous. A timely identification of such newly developing critical situations represents a challenge in hazard assessment.

Acknowledgments

This work was partly supported by the European Union Seventh Framework Program's (EU-FP7) project Assessing Climate impacts on the Quantity and quality of WAter (ACQWA; grant 212250). We wish to thank "Fondazione Montagna Sicura" (Aoste, Italy) for their monitoring of Grandes Jorasses glacier. The authors acknowledge helpful discussions and exchanges with Fabian Walter. The authors thank also Martin Truffer, Roderik van de Wal, and the Editor for their useful comments that significantly improved the manuscript, and Jérome Smith for proofreading the English. Data to support this article are available upon request from the author (jerome.faillettaz@geo.uzh.ch).

The Editor on this paper was Eelco Rohling. He thanks Martin Truffer, Roderik van del Wal, and one anonymous reviewer for their review assistance on this manuscript

References

Alava, M. J., P. K. V. V. Nukala, and S. Zapperi (2006), Statistical models of fracture, *Adv. Phys.*, *55*(3-4), 349–476, doi:10.1080/00018730300741518.

Alean, J. (1985), Ice avalanches: Some empirical information about their formation and reach, *J. Glaciol.*, *31*(109), 324–333.

Alley, R. B., H. J. Horgan, I. Joughin, K. M. Cuffey, T. K. Dupont, B. R. Parizek, S. Anandakrishnan, and J. Bassis (2008), A simple law for ice-shelf calving, *Science*, *322*(5906), 1344, doi:10.1126/science.1162543.

Allstadt, K., and S. D. Malone (2014), Swarms of repeating stick-slip icequakes triggered by snow loading at Mount Rainier volcano, *J. Geophys. Res. Earth Surf.*, *119*, 1180–1203, doi:10.1002/2014JF003086.

Amitrano, D., J. R. Grasso, and G. Senfaute (2005), Seismic precursory patterns before a cliff collapse and critical point phenomena, *Geophys. Res. Lett.*, *32*, L08314, doi:10.1029/2004GL022270.

Amundson, J. M., M. Truffer, M. P. Lüthi, M. Fahnestock, M. West, and R. J. Motyka (2008), Glacier, fjord, and seismic response to recent large calving events, Jakobshavn Isbrae, Greenland, *Geophys. Res. Lett.*, *35*, L22501, doi:10.1029/2008GL035281.

Andersen, J. V., D. Sornette, and K.-t. Leung (1997), Tricritical behavior in rupture induced by disorder, *Phys. Rev. Lett.*, *78*, 2140–2143, doi:10.1103/PhysRevLett.78.2140.

Anifrani, J.-C., C. Le Floc'h, D. Sornette, and B. Souillard (1995), Universal log-periodic correction to renormalization group scaling for rupture stress prediction from acoustic emissions, *J. Phys. I Fr.*, *5*(6), 631–638, doi:10.1051/jp1:1995156.

Åström, J., et al. (2014), Termini of calving glaciers as self-organized critical systems, *Nat. Geosci.*, *7*(12), 874–878, doi:10.1038/NGEO2290.

Bartholomaus, T. C., C. F. Larsen, S. O'Neel, and M. E. West (2012), Calving seismicity from iceberg-sea surface interactions, *J. Geophys. Res.*, *117*, F04029, doi:10.1029/2012JF002513.

Bassis, J. (2011), The statistical physics of iceberg calving and the emergence of universal calving laws, *J. Glaciol.*, *57* (201), 3–16, doi:10.3189/002214311795306745.

Benn, D. I., C. R. Warren, and R. H. Mottram (2007a), Calving processes and the dynamics of calving glaciers, *Earth Sci. Rev.*, *82*(3–4), 143–179, doi:10.1016/j.earscirev.2007.02.002.

Benn, D. I., N. R. Hulton, and R. H. Mottram (2007b), 'Calving laws', 'sliding laws' and the stability of tidewater glaciers, *Ann. Glaciol.*, *46*(1), 123–130.

Boulton, G., R. Lunn, P. Vidstrand, and S. Zatsepin (2007), Subglacial drainage by groundwater-channel coupling, and the origin of esker systems: Part 1. Glaciological observations, *Quat. Sci. Rev.*, *26*(7-8), 1067–1090, doi:10.1016/j.quascirev.2007.01.007.

Bowman, D. D., G. Ouillon, C. G. Sammis, A. Sornette, and D. Sornette (1998), An observational test of the critical earthquake concept, *J. Geophys. Res.*, *103*(B10), 24,359–24,372, doi:10.1029/98JB00792.

Bufe, C. G., and D. J. Varnes (1993), Predictive modeling of the seismic cycle of the greater San Francisco Bay region, *J. Geophys. Res.*, *98*(B6), 9871–9883, doi:10.1029/93JB00357.

Clauset, A., C. Shalizi, and M. Newman (2009), Power-law distributions in empirical data, *SIAM Rev.*, *51*(4), 661–703, doi:10.1137/070710111.

Cook, S., I. Rutt, T. Murray, A. Luckman, T. Zwinger, N. Selmes, A. Goldsack, and T. James (2014), Modelling environmental influences on calving at Helheim Glacier in Eastern Greenland, *The Cryosphere*, *8*(3), 827–841.

Dalban Canassy, P., A. Bauder, M. Dost, R. Fäh, M. Funk, S. Margreth, B. Müller, and S. Sugiyama (2011), Hazard assessment investigations due to the recent changes in Triftgletscher, *Nat. Hazard Earth Syst.*, *11*, 2149–2162.

Dalban Canassy, P., J. Faillettaz, F. Walter, and M. Huss (2012), Seismic activity and surface motion of a steep temperate glacier: A study on Triftgletscher, Switzerland, *J. Glaciol.*, *58*(209), 513–528, doi:10.3189/2012JoG11J104.

Dalban Canassy, P., F. Walter, S. Husen, H. Maurer, J. Faillettaz, and D. Farinotti (2013), Investigating the dynamics of an alpine glacier using probabilistic icequake locations: Triftgletscher, Switzerland, *J. Geophys. Res. Earth Surf.*, *118*, 2003–2018, doi:10.1002/jgrf.20097.

Deichmann, N., J. Ansorge, F. Scherbau, A. Aschwanden, F. Bernhardi, and G. H. Gudmundsson (2000), Evidence for deep icequakes in an alpine glacier, *Ann. Glaciol.*, *31*, 85–90.

Dieterich, J. (1994), A constitutive law for rate of earthquake production and its application to earthquake clustering, *J. Geophys. Res.*, *99*(B2), 2601–2618, doi:10.1029/93JB02581.

Dixon, N., R. Hill, and J. Kavanagh (2003), Acoustic emission monitoring of slope instability: Development of an active waveguide system, in *Proceedings of the Institution of Civil Engineers - Geotechnical Engineering*, vol. 156, pp. 83–95, Thomas Telford, London.

Dixon, N., and M. Spriggs (2007), Quantification of slope displacement rates using acoustic emission monitoring, *Can. Geotech. J.*, *44*, 966–976.

Du Pasquier, L. (1896), L'avalanche du glacier de l'Altels le 11 Septembre 1895, *Ann. Geophys.*, *5*(23), 458–468.

Ekström, G., M. Nettles, and G. A. Abers (2003), Glacial earthquakes, *Science*, *302*(5645), 622–624, doi:10.1126/science.1088057.

Ekström, G., M. Nettles, and V. C. Tsai (2006), Seasonality and increasing frequency of Greenland glacial earthquakes, *Science*, *311*(5768), 1756–1758, doi:10.1126/science.1122112.

Evans, S., O. Tutubalina, V. Drabyshev, S. Chernomorets, S. McDougall, D. Petrakov, and O. Hungr (2009), Catastrophic detachment and high-velocity long-runout flow of Kolka glacier, Caucasus mountains, Russia in 2002, *Geomorphology*, *105*, 314–321, doi:10.1016/j.geomorph.2008.10.008.

Faillettaz, J., A. Pralong, M. Funk, and N. Deichmann (2008), Evidence of log-periodic oscillations and increasing icequake activity during the breaking-off of large ice masses, *J. Glaciol.*, *54*(187), 725–737, doi:10.3189/002214308786570845.

Faillettaz, J., D. Sornette, and M. Funk (2010), Gravity-driven instabilities: Interplay between state-and-velocity dependent frictional sliding and stress corrosion damage cracking., *J. Geophys. Res.*, *115*, B03409, doi:10.1029/2009JB006512.

Faillettaz, J., D. Sornette, and M. Funk (2011a), Numerical modeling of a gravity-driven instability of a cold hanging glacier: Reanalysis of the 1895 break-off of Altelsgletscher, Switzerland, *J. Glaciol.*, *57*(205), 817–831, doi:10.3189/002214311798043852.

Faillettaz, J., M. Funk, and D. Sornette (2011b), Icequakes coupled with surface displacements for predicting glacier break-off, *J. Glaciol.*, *57*(203), 453–460, doi:10.3189/002214311796905668.

Faillettaz, J., M. Funk, and D. Sornette (2012), Instabilities on alpine temperate glaciers: New insights arising from the numerical modelling of Allalingletscher (Valais, Switzerland), *Nat. Hazard Earth Syst.*, *12*(9), 2977–2991, doi:10.5194/nhess-12-2977-2012.

Flotron, A. (1977), Movement studies on hanging glaciers in relation with an ice avalanche, *J. Glaciol.*, *19*(81), 671–672.

Forel, F. A. (1895), L'éboulement du glacier de l'Altels. Archive des sciences physiques et naturelles, *Genève*, *34*, 513–543.

Gilbert, A., and C. Vincent (2013), Atmospheric temperature changes over the 20th century at very high elevations in the European Alps from englacial temperatures, *Geophys. Res. Lett.*, *40*, 2102–2108, doi:10.1002/grl.50401.

Gilbert, A., O. Gagliardini, C. Vincent, and P. Wagnon (2014), A 3-D thermal regime model suitable for cold accumulation zones of polythermal mountain glaciers, *J. Geophys. Res. Earth Surf.*, *119*, 1876–1893, doi:10.1002/2014JF003199.

Glaister, R. M. (1951), The ice slide on the Glacier du Tour, *J. Glaciol.*, *1*(9), 508–509.

Griffith, A. A. (1921), The Phenomena of Rupture and Flow in Solids, *Philos. Trans. R. Soc. London*, *A221*, 163–198.

Haeberli, W., C. Huggel, A. Kääb, S. Zgraggen-Oswald, A. Polkvoj, I. Galushkin, I. Zotikov, and N. Osokin (2004), The Kolka-Karmadon rock/ice slide of 20 September 2002: An extraordinary event of historical dimensions in North Ossetia, Russian Caucasus, *J. Glaciol.*, *50*(171), 533–546, doi:10.3189/172756504781829710.

Hanson, B., and R. L. Hooke (2000), Glacier calving: A numerical model of forces in the calving-speed/water-depth relation, *J. Glaciol.*, *46*(153), 188–196.

Heim, A. (1895), *Die Gletscherlawine an der Altels am 11. September 1895*, Zürcher und Furrer, Zürich.

Huang, Y., G. Ouillon, H. Saleur, and D. Sornette (1997), Spontaneous generation of discrete scale invariance in growth models, *Phys. Rev. E*, *55*(6), 6433–6447.

Huggel, C., W. Haeberli, A. Kääb, D. Bieri, and S. Richardson (2004), Assessment procedures for glacial hazards in the Swiss Alps, *Can. Geotech. J.*, *41*(6), 1068–1083.

Huggel, C., S. Zgraggen-Oswald, W. Haeberli, A. Kääb, A. Polkvoj, I. Galushkin, and S. G. Evans (2005), The 2002 rock/ice avalanche at Kolka/Karmadon, Russian Caucasus: Assessment of extraordinary avalanche formation and mobility, and application of quickbird satellite imagery, *Nat. Hazard Earth Syst.*, *5*(2), 173–187, doi:10.5194/nhess-5-173-2005.

Ide, K., and D. Sornette (2002), Oscillatory finite-time singularities in finance, population and rupture, *Physica A*, *307*(1-2), 63–106.

Irvine-Fynn, T. D. L., A. J. Hodson, B. J. Moorman, G. Vatne, and A. L. Hubbard (2011), Polythermal glacier hydrology: A review, *Rev. Geophys.*, *49*, RG4002, doi:10.1029/2010RG000350.

Jaumé, S. C., and L. R. Sykes (1999), Evolving towards a critical point: A review of accelerating seismic moment/energy release prior to large and great earthquakes, *Pure Appl. Geophys.*, *155*, 279–305, doi:10.1007/s000240050266.

Jay-Allemand, M., F. Gillet-Chaulet, O. Gagliardini, and M. Nodet (2011), Investigating changes in basal conditions of Variegated Glacier prior to and during its 1982–1983 surge, *The Cryosphere*, *5*, 659–672, doi:10.5194/tc-5-659-2011.

Johansen, A., and D. Sornette (2000), Critical ruptures, *Eur. Phys. J. B*, *18*(1), 163–181, doi:10.1007/s100510070089.

Johansen, A., and D. Sornette (2001), Finite-time singularity in the dynamics of the world population, economic and financial indices, *Physica A*, *294*(3-4), 465–502.

Kolesnikov, Yu. I., M. M. Nemirovich-Danchenko, S. V. Goldin, and V. S. Seleznev (2003), Slope stability monitoring from microseismic field using polarization methodology, *Nat. Hazard Earth Syst. Sci.*, *3*, 515–521.

Krug, J., J. Weiss, O. Gagliardini, and G. Durand (2014), Combining damage and fracture mechanics to model calving, *Cryosphere Discuss.*, *8*(2), 2101–2117, doi:10.5194/tcd-8-2101-2014.

Kuksenko, V., N. Tomilin, and A. Chmel (2005), The role of driving rate in scaling characteristics of rock fracture, *J. Stat. Mech: Theory Exp.*, *2005*(06), P06012, doi:10.1088/1742-5468/2005/06/P06012.

Le Meur, E., and C. Vincent (2006), Monitoring of the Taconnaz ice fall (French Alps) using measurements of mass balance, surface velocities and ice cliff position, *Cold Reg. Sci. Technol.*, *46*(1), 1–11, doi:10.1016/j.coldregions.2006.05.001.

Lliboutry, L. (1975), La catastrophe du Yungay (Pérou), *Proceedings of the Snow and Ice Symposium, Moscow, August 1971*, pp. 353–363.

MacAyeal, D. R., E. A. Okal, R. C. Aster, and J. N. Bassis (2008), Seismic and hydroacoustic tremor generated by colliding icebergs, *J. Geophys. Res.*, *113*, F03011, doi:10.1029/2008JF001005.

Mahrenholtz, O., and Z. Wu (1992), Determination of creep damage parameters for polycrystalline ice, *Advances in Ice Technology (3rd Int. Conf. Ice Tech./Cambridge USA)*, pp. 181–192.

Margreth, S., J. Faillettaz, M. Funk, M. Vagliasindi, F. Diotri, and M. Broccolato (2011), Safety concept for hazards caused by ice avalanches from Whymper hanging glacier in the Mont-Blanc massif., *Cold Reg. Sci. Technol.*, *69*(2-3), 194–201, doi:10.1016/j.coldregions.2011.03.006.

Moore, J. C., A. Grinsted, T. Zwinger, and S. Jevrejeva (2013), Semiempirical and process-based global sea level projections, *Rev. Geophys.*, *51*, 484–522, doi:10.1002/rog.20015.

Neave, K. G., and J. C. Savage (1970), Icequakes on the Athabasca glacier, *J. Geophys. Res.*, *75*(8), 1351–1362, doi:10.1029/JB075i008p01351.

Nechad, H., A. Helmstetter, R. El Guerjouma, and D. Sornette (2005a), Andrade and critical time-to-failure laws in fiber-matrix composites: Experiments and model, *J. Mech. Phys. Solids*, *53*, 1099–1127.

Nechad, H., A. Helmstetter, R. El Guerjouma, and D. Sornette (2005b), Creep rupture in heterogeneous materials, *Phys. Rev. Lett.*, *94*, 045501.

Nettles, M., et al. (2008), Step-wise changes in glacier flow speed coincide with calving and glacial earthquakes at Helheim glacier, Greenland, *Geophys. Res. Lett.*, *35*, L24503, doi:10.1029/2008GL036127.

O'Neel, S., H. P. Marshall, D. E. McNamara, and W. T. Pfeffer (2007), Seismic detection and analysis of icequakes at Columbia Glacier, Alaska, *J. Geophys. Res.*, *112*, F03S23, doi:10.1029/2006JF000595.

O'Neel, S., and W. T. Pfeffer (2007), Source mechanics for monochromatic icequakes produced during iceberg calving at Columbia Glacier, AK, *Geophys. Res. Lett.*, *34*, L22502, doi:10.1029/2007GL031370.

Pralong, A. (2006), Oscillations in critical shearing, application to fractures in glaciers, *Nonlinear Processes Geophys.*, *13*, 681–693.

Pralong, A., and M. Funk (2005), Dynamic damage model of crevasse opening and application to glacier calving, *J. Geophys. Res.*, *110*, B01309, doi:10.1029/2004JB003104.

Pralong, A., and M. Funk (2006), On the instability of avalanching glaciers, *J. Glaciol.*, *52*(176), 31–48, doi:10.3189/172756506781828980.

Pralong, A., C. Birrer, W. A. Stahel, and M. Funk (2005), On the predictability of ice avalanches, *Nonlinear Processes Geophys.*, *12*(6), 849–861, doi:10.5194/npg-12-849-2005.

Pralong, A., K. Hutter, and M. Funk (2006), Anisotropic damage mechanics for viscoelastic ice, *Continuum Mech. Thermodyn.*, *17*(5), 387–408, doi:10.1007/s00161-005-0002-5.

Press, W. (1996), *Numerical Recipes in Fortran 90: Volume 2, Volume 2 of Fortran Numerical Recipes: The Art of Parallel Scientific Computing*, Fortran Numerical Recipes, Cambridge Univ. Press, Cambridge, U. K.

Qamar, A. (1988), Calving icebergs: A source of low-frequency seismic signals from Columbia glacier, Alaska, *J. Geophys. Res.*, *93*(B6), 6615–6623, doi:10.1029/JB093iB06p06615.

Raymond, M., M. Wegmann, and M. Funk (2003), *Inventar gefährlicher Gletscher in der Schweiz*, Mitteilung, 182, VAW, ETH Zürich.

Reeh, N. (1968), On the calving of ice from floating glaciers and ice shelves, *J. Glaciol.*, *7*(50), 215–232.

Röthlisberger, H. (1955), Studies in glacier physics on the Penny Ice Cap, Baffin Island, 1953, Part III: Seismic sounding, *J. Glaciol.*, *2*(18), 539–552, doi:10.3189/002214355793702064.

Röthlisberger, H. (1981), Eislawinen und Ausbrüche von Gletscherseen, in *Gletscher und Klima - glaciers et climat, Jahrbuch der Schweizerischen Naturforschenden Gesellschaft, wissenschaftlicher Teil 1978*, edited by P. Kasser, pp. 170–212, Birkhäuser Verlag Basel, Boston, Stuttgart.

Röthlisberger, H., and P. Kasser (1978), The readvance of the Allalingletscher after the ice avalanche of 1965, *Materialy Glyatsiologicheskikh Issledovaniy. Khronika Obsuzhdeniya*, *33*, 152–164.

Roux, P. F., D. Marsan, J-P. Metaxian, G. O'Brien, and L. Moreau (2008), Microseismic activity within a serac zone in an alpine glacier (Glacier d'Argentière, Mont-Blanc, France), *J. Glaciol.*, *54*(184), 157–168.

Ruina, A. (1983), Slip instability and state variable friction laws, *J. Geophys. Res.*, *88*(B12), 10,359–10,370, doi:10.1029/JB088iB12p10359.

Sahimi, M., and S. Arbabi (1996), Scaling laws for fracture of heterogeneous materials and rock, *Phys. Rev. Lett.*, *77*, 3689–3692, doi:10.1103/PhysRevLett.77.3689.

Sammis, S. G., and D. Sornette (2002), Positive feedback, memory and the predictability of earthquakes, *Proc. Natl. Acad. Sci. USA*, *99*(SUPP1), 2501–2508.

Schweizer, J., and A. Iken (1992), The role of bed separation and friction in sliding over an undeformable bed, *J. Glaciol.*, *38*(128), 77–92.

Sornette, D. (1998), Discrete-scale invariance and complex dimensions, *Phys. Rep.*, *297*(5), 239–270, doi:10.1016/S0370-1573(97)00076-8.

Sornette, D. (2006), *Critical Phenomena in Natural Sciences: Chaos, Fractals, Self-organization and Disorder: Concepts and Tools*, Springer Series in Synergetics, Springer, Berlin, doi:10.1007/3-540-33182-4.

Sornette, A., and D. Sornette (1990), Earthquake rupture as a critical point: Consequences for telluric precursors, *Tectonophysics*, *179*(3-4), 327–334, doi:10.1016/0040-1951(90)90298-M.

Sornette, D., and J. Andersen (1998), Scaling with respect to disorder in time-to-failure, *Eur. Phys. J. B*, *1*(3), 353–357, doi:10.1007/s100510050194.

Sornette, D., and C. G. Sammis (1995), Complex critical exponents from renormalization group theory of earthquakes: Implications for earthquake predictions, *J. Phys. I Fr.*, *5*(5), 607–619, doi:10.1051/jp1:1995154.

Sornette, D., and C. Vanneste (1992), Dynamics and memory effects in rupture of thermal fuse networks, *Phys. Rev. Lett.*, *68*, 612–615, doi:10.1103/PhysRevLett.68.612.

Sornette, D., A. Helmstetter, J. Andersen, S. Gluzman, J.-R. Grasso, and V. Pisarenko (2004), Towards landslide predictions: Two case studies, *Physica A*, *338*(3-4), 605–632, doi:10.1016/j.physa.2004.02.065.

St. Lawrence, W., and A. Qamar (1979), Hydraulic transients: A seismic source in volcanoes and glaciers, *Science*, *203*(4381), 654–656, doi:10.1126/science.203.4381.654.

Todd, J., and P. Christoffersen (2014), Are seasonal calving dynamics forced by buttressing from ice mélange or undercutting by melting? Outcomes from full-Stokes simulations of Store Glacier, West Greenland, *The Cryosphere*, *8*, 2353–2365, doi:10.5194/tc-8-2353-2014.

Van der Veen, C. J. (1999), Crevasses on glaciers, *Polar Geog.*, *23*(3), 213–245, doi:10.1080/10889379909377677.

Van der Veen, C. J. (2002), Calving glaciers, *Prog. Phys. Geog.*, *26*(1), 96–122, doi:10.1191/0309133302pp327ra.

Vincent, C., E. Le Meur, D. Six, P. Possenti, E. Lefebvre, and M. Funk (2007), Climate warming revealed by englacial temperatures at Col du Dôme (4250 m, Mont Blanc area), *Geophys. Res. Lett.*, *34*, L16502, doi:10.1029/2007GL029933.

Vincent, C., M. Descloitres, S. Garambois, A. Legchenko, H. Guyard, and A. Gilbert (2012), Detection of a subglacial lake in the Tête Rousse glacier (Mont Blanc area), *J. Glaciol.*, *58*(211), 866–878, doi:10.3189/2012JoG11J179.

Vincent, C., E. Thibert, M. Harter, A. Soruco, and A. Gilbert (2015), Volume and frequency of ice avalanches from the Taconnaz hanging glacier (French Alps), *Ann. Glaciol.*, *56*(70), 17–25.

Voight, B. (1988), A method for prediction of volcanic eruptions, *Nature*, *332*(6160), 125–130.

Voight, B. (1989), A relation to describe rate-dependent material failure, *Science*, *243*(4888), 200–203.

Walter, F., N. Deichmann, and M. Funk (2008), Basal icequakes during changing subglacial water pressures beneath Gornergletscher, Switzerland, *J. Glaciol.*, *54*(186), 511–521, doi:10.3189/002214308785837110.

Walter, F., S. O'Neel, D. McNamara, W. T. Pfeffer, J. N. Bassis, and H. A. Fricker (2010), Iceberg calving during transition from grounded to floating ice: Columbia Glacier, Alaska, *Geophys. Res. Lett.*, *37*, L15501, doi:10.1029/2010GL043201.

Walter, F., J. M. Amundson, S. O'Neel, M. Truffer, M. Fahnestock, and H. A. Fricker (2012), Analysis of low-frequency seismic signals generated during a multiple-iceberg calving event at Jakobshavn Isbrae, Greenland, *J. Geophys. Res.*, *117*, F01036, doi:10.1029/2011JF002132.

Weaver, C., and S. Malone (1979), Seismic evidence for discrete glacier motion at the rock-ice interface, *J. Glaciol.*, *23*(89), 171–184.

West, M. E., C. F. Larsen, M. Truffer, S. O'Neel, and L. LeBlanc (2010), Glacier microseismicity, *Geology*, *38*(4), 319–322, doi:10.1130/G30606.1.

Weiss, J. (2004), Subcritical crack propagation as a mechanism of crevasse formation and iceberg calving, *J. Glaciol.*, *50*(168), 109–115, doi:10.3189/172756504781830240.

Wiens, D. A., S. Anandakrishnan, J. P. Winberry, and M. A. King (2008), Simultaneous teleseismic and geodetic observations of the stick-slip motion of an Antarctic ice stream, *Nature*, *453*(7196), 770–774, doi:10.1038/nature06990.

Winberry, J. P., S. Anandakrishnan, D. A. Wiens, and R. B. Alley (2013), Nucleation and seismic tremor associated with the glacial earthquakes of Whillans Ice Stream, Antarctica, *Geophys. Res. Lett.*, *40*, 312–315, doi:10.1002/grl.50130.

Zhou, W.-X., and D. Sornette (2002a), Evidence of intermittent cascades from discrete hierarchical dissipation in turbulence, *Physica D*, *165*(1-2), 94–125, doi:10.1016/S0167-2789(02)00390-1.

Zhou, W.-X., and D. Sornette (2002b), Generalized q analysis of log-periodicity: Applications to critical ruptures, *Phys. Rev. E*, *66*, 046111, doi:10.1103/PhysRevE.66.046111.